

Static Black Hole Solution with a Dark Matter Halo

Uktamjon Uktamov,^{1,*} Sanjar Shaymatov,^{1,2,†} and Bobomurat Ahmedov^{1,3,4,5,‡}

¹*Institute of Fundamental and Applied Research,
National Research University TIIAME, Kori Niyoziy 39, Tashkent 100000, Uzbekistan*

²*Institute for Theoretical Physics and Cosmology,
Zhejiang University of Technology, Hangzhou 310023, China*

³*School of Physics, Harbin Institute of Technology, Harbin 150001, People's Republic of China*

⁴*Institute for Advanced Studies, New Uzbekistan University,
Movarounnahr str. 1, Tashkent 100000, Uzbekistan*

⁵*Institute of Theoretical Physics, National University of Uzbekistan, Tashkent 100174, Uzbekistan*
(Dated: June 15, 2025)

In this letter, we present a novel analytical Schwarzschild-like black hole (BH) solution that exhibits a static BH with a dark matter (DM) halo characterized by a Dehnen-type density profile. We study the properties of the newly derived BH solution by examining its spacetime curvature characteristics and energy conditions, providing insights into how the DM halo influences these fundamental characteristics. This solution could represent an alternative perspective on the interaction of black hole-dark matter systems, providing new insights into the fundamental properties of DM halos.

I. INTRODUCTION

In general relativity (GR), black holes (BHs) arise naturally as exact solutions to Einstein's gravitational field equations. These theoretical predictions were made a long time back; nearly a century later, observational evidence for the existence of BHs was found through modern revolutionary Event Horizon Telescope (EHT) and LIGO-VIRGO observations [1–4]. These triumphal observations are expected to provide stringent tests that probe the nature and unknown aspects of BHs. However, open questions remain regarding the behavior of BHs and their interaction with their surroundings. Among them, the nature and existence of dark matter are long-standing problems in GR. Consequently, identifying evidence for dark matter (DM) within the BH environment has become a crucial task in GR.

In many astrophysical scenarios, supermassive BHs at the centers of galaxies are believed to be enveloped by matter distributions, including DM halos. It is well established that BHs are characterized by complex and dynamic environments, and there is substantial evidence to suggest that supermassive BHs at the center of most galaxies are the primary drivers of active galactic nuclei [5, 6] and are surrounded by a DM halo [7, 8]. In addition to the possibility of DM enveloping supermassive BHs, considerable evidence suggests that DM significantly influences galactic rotation curves [9], bullet clusters [10], and the large-scale structure of the universe [11].

The discovery of unexpectedly flat galactic rotation curves in large spiral and elliptical galaxies led to the postulation of the existence of DM. This DM, now supported by extensive astrophysical observations, is esti-

mated to constitute approximately 90% of the mass of a galaxy, the remaining 10% being luminous baryonic matter [12]. Initially concentrated near galactic centers, facilitating star formation and clustering, dark matter gradually migrated outward during galactic evolution, forming DM halos around the galaxy through various dynamical processes. Astrophysical observations reveal that many large spiral and elliptical galaxies harbor a central supermassive BH (sometimes binary systems) embedded within this DM halo [3, 4, 13, 14]. A substantial amount of DM in our universe is necessary to provide a satisfactory explanation for the observed phenomena. This is supported by cosmic microwave background observations, which reveal that DM comprises roughly 27% of the universe, alongside 68% dark energy. The rest of the universe, only around 5%, is considered normal matter. Numerous theoretical particle candidates, predicted by extensions of the standard-model, are being investigated as potential components of DM [15–18], such as weakly interacting massive particles (WIMPs), axions, and sterile neutrinos. With this in view, properties of DM can then be probed gravitationally in the case of weak interaction within standard-model particles. Therefore, DM may be highly concentrated around supermassive BHs, commonly found in galactic centers [7, 8], significantly influencing extreme [19] and intermediate [20, 21] mass ratio inspirals and potentially revealing the distribution of the DM halo. The influence of DM halos on supermassive BHs is a critical area of research, driven by the need to understand the DM-BH interaction. DM halo structures demonstrably affect galactic rotation curves [8–10] and dynamics observed in events such as the Bullet Cluster collision [22]. Although current models primarily describe DM as interacting gravitationally, a substantial body of evidence convincingly supports its existence [23–25].

Motivated by these findings, it is important to analyze the DM-BH interaction and look for DM models to help

* uktam.uktamov11@gmail.com

† sanjar@astrin.uz

‡ ahmedov@astrin.uz

improve our understanding of the fundamental nature of DM. Given this fundamental importance of DM halos and their interaction with BH systems, the exploration and analysis of DM models can yield valuable insights, relying on astrophysical data and simulation studies. Motivated by this, several analytical models have been developed to describe BH solutions within DM halos, including the Einasto [26, 27], Navarro-Frenk-White [28], and Burkert [29] models, as well as the Dehnen model [30–34]. Additionally, some models incorporate a DM profile linked to a phantom scalar field [35–38]. Furthermore, analytical models exhibiting supermassive BH solutions embedded in a DM halo have also been investigated in Refs. [39–41].

Investigations within the Dehnen-type DM halo model have also explored DM-BH interactions from various perspectives. For instance, one study examined the influence of density profile slopes on the survival of low star formation efficiency star clusters after rapid gas expulsion [31]. Other scenarios have also considered star clusters with Plummer and Dehnen profiles, focusing on differing slope cusps at the time of formation. Furthermore, the BH-Dehnen-type DM halo solution has been proposed to investigate ultra-faint dwarf galaxies [33]. Recent studies have also introduced new BH solutions surrounded by Dehnen-type DM halos [32, 34], using Schwarzschild BH within the halo environment. Thermodynamics and null geodesics of the effective BH-DM halo system were analyzed [32], with a subsequent study constraining the DM halo parameters [42]. Finally, the impact of the DM halo on quasinormal modes, the photon sphere radius and the BH shadow [43, 44], as well as gravitational waveforms from periodic orbits [45], were investigated within the solution of the BH-Dehnen DM halo [34].

In this letter, we derive a new Schwarzschild-like BH solution immersed in a DM halo characterized by a Dehnen-type density profile $(1, 4, 2)$. To accomplish this, we adopt the method developed in [46, 47]. We first analyze the spacetime curvature invariants and subsequently investigate the associated energy conditions. Finally, we explore the influence of the DM profile on timelike particle geodesics, providing deeper insights into how the DM halo affects particle geodesics.

The structure of this letter is organized as follows: In Sec. II, we present a new Schwarzschild-like BH solution surrounded by a DM halo with a Dehnen-type density profile $(1, 4, 2)$. In Sec. III, we investigate the spacetime curvature invariants and analyze the corresponding energy conditions. Finally, we summarize our findings and conclusions in Sec. IV.

II. SCHWARZSCHILD-LIKE BLACK HOLE SPACETIME WITH THE DARK MATTER HALO

Here, we consider a Schwarzschild-like BH spacetime surrounded a DM halo characterized by a Dehnen-type density profile. We first consider a background space-

time involving the DM distribution and then derive the BH-DM solution by solving Einstein's field equations. In this case, a Schwarzschild BH can be considered with a Dehnen-type DM halo mass distribution. This is determined by the DM density distribution (see details in Ref. [48]). With this approach, we start by describing the spacetime geometry with the DM halo first and then include the Schwarzschild BH spacetime geometry. Now, we write the general form of the density profile in order to further derive the Dehnen-type DM halo mass distribution, which is defined by

$$\rho(r) = \rho_s \left(\frac{r}{r_s}\right)^{-\gamma} \left[\left(\frac{r}{r_s}\right)^\alpha + 1\right]^{\frac{\gamma-\beta}{\alpha}}, \quad (1)$$

where ρ_s and r_s are the characteristic density and characteristic scale of the DM halo, respectively. It must be emphasized that, apart from the characteristic DM halo parameters, α , β and γ are specific parameters of the density profile. For example, γ can range only from 0 to 3. In this work, we use the following Dehnen-type density distribution $(\alpha, \beta, \gamma) = (1, 4, 2)$ for the DM halo. Taken together with Eq. (1), we derive the mass profile as follows:

$$M_D(r) = \int_0^r 4\pi\rho(r_1)r_1^2 dr_1 = \frac{4\pi\rho_s r_s^3}{1 + \frac{r_s}{r}}. \quad (2)$$

We then define the line element of the DM halo, including redshift $A(r)$ and shape $B(r)$ functions, which is given by

$$ds^2 = -A(r)dt^2 + \frac{dr^2}{B(r)} + r^2 d\Omega^2, \quad (3)$$

where $d\Omega^2 = d\theta^2 + \sin^2\theta d\phi^2$ is referred to as the solid angle in spherical coordinates. The point to be noted here is that $A(r)$ can be used to define the tangential velocity of particles moving within the DM halo as follows:

$$v_D^2 = \frac{1}{r} \partial_r \left(\log \sqrt{A(r)} \right) = \frac{M_D}{r}, \quad (4)$$

which enables us to determine $A(r)$ as

$$\begin{aligned} A(r) &= \left(1 + \frac{r_s}{r}\right)^{-8\pi r_s^2 \rho_s} \\ &\approx 1 - \frac{2M_D(r)}{r_s} \left(1 + \frac{r_s}{r}\right) \log \left(1 + \frac{r_s}{r}\right). \end{aligned} \quad (5)$$

For the DM halo itself (3), the Einstein field equation yields as ([34, 47]):

$$R_{\mu\nu} - \frac{1}{2}g_{\mu\nu}R = 8\pi T_{\mu\nu}(D), \quad (6)$$

where the source part $T_{\mu\nu}(D)$ is given by

$$T_{\mu}^{\nu}(D) = g^{\nu\alpha}T_{\mu\alpha}(D) = \text{diag}[-\rho(r), P_r(r), P_t(r), P_t(r)],$$

which stands for the energy-momentum tensor of the Dehnen type DM halo spacetime. Similarly, the line element for the BH spacetime, including the DM halo, can

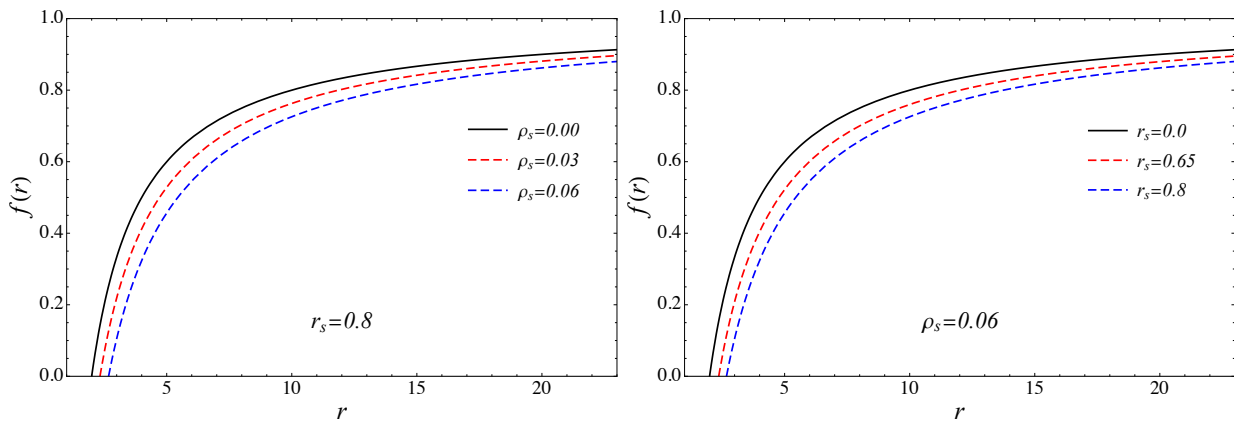


FIG. 1: Radial profile of function $f(r)$ for various values of the characteristic density ρ_s and characteristic scale r_s of the DM halo. Hereafter, we shall for simplicity set $M = 1$.

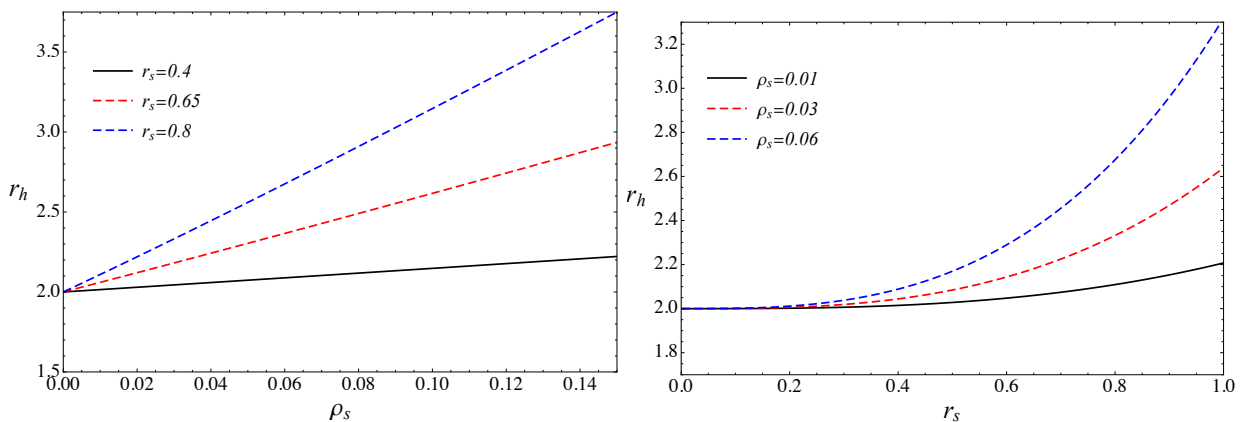


FIG. 2: The dependence of BH event horizon on the density ρ_s and the characteristic scale r_s of the DM halo.

be written as a result of the combined BH-DM halo system

$$ds^2 = -[A(r) + F_1(r)] dt^2 + \frac{dr^2}{B(r) + F_2(r)} + r^2 d\Omega^2, \quad (7)$$

for which the Einstein field equation reads

$$R_{\mu\nu} - \frac{1}{2}g_{\mu\nu}R = 8\pi [T_{\mu\nu}(D) + T_{\mu\nu}(BH)], \quad (8)$$

with the energy-momentum tensor $T_{\mu\nu}(BH)$ of the BH spacetime. For the combined BH-DM halo system, Einstein field equations can be written as follows: (6,8) and line elements (3,7) we will have:

$$\begin{aligned} [B(r) + F_2(r)] \left[\frac{1}{r} \frac{B'(r) + F_2'(r)}{B(r) + F_2(r)} + \frac{1}{r^2} \right] \\ = B(r) \left[\frac{1}{r} \frac{B'(r)}{B(r)} + \frac{1}{r^2} \right], \end{aligned} \quad (9)$$

$$\begin{aligned} [B(r) + F_2(r)] \left[\frac{1}{r} \frac{A'(r) + F_1'(r)}{A(r) + F_1(r)} + \frac{1}{r^2} \right] \\ = B(r) \left[\frac{1}{r} \frac{A'(r)}{A(r)} + \frac{1}{r^2} \right]. \end{aligned} \quad (10)$$

Consequently, the above equations lead to the space-time metric, including the DM halo, which can be written as

$$\begin{aligned} ds^2 = - \exp \left[\int \frac{B(r)}{B(r) - \frac{2M}{r}} \left(\frac{1}{r} + \frac{A'(r)}{A(r)} \right) dr \right] dt^2 \\ - A(r) dt^2 + \frac{dr^2}{B(r) - \frac{2M}{r}} + r^2 (d\theta^2 + \sin^2 \theta d\phi^2), \end{aligned} \quad (11)$$

It must be emphasized that one can recover $A(r) = B(r) = 1$ in the case of vanishing DM halo, the resulting integral gives $(1 - \frac{2M}{r})$ that exhibits the Schwarzschild BH solution with the mass M . As a result, Eqs. (9) and (10) solve to give

$$F_1(r) = \exp \left[\int \left(\frac{B(r)}{B(r) + F_2(r)} \left(\frac{1}{r} + \frac{A'(r)}{A(r)} \right) - \frac{1}{r} \right) dr \right] - A(r), \quad (12)$$

$$F_2(r) = -\frac{2M}{r}, \quad (13)$$

where prime $'$ denotes derivative with respect to r . At this stage, we shall for simplicity consider the condition

$A(r) = B(r)$, leading to the resulting spacetime metric describing the Schwarzschild-like BH with the DM halo characterized by the Dehnen-type density distribution profile (1, 4, 2). The resulting spacetime metric derived as the exact solution of the field equations (6) reads as

$$ds^2 = -f(r)dt^2 + \frac{1}{f(r)}dr^2 + r^2(d\theta^2 + \sin^2\theta d\phi^2), \quad (14)$$

where

$$f(r) = 1 - \frac{2M}{r} - \frac{8\pi\rho_s r_s^2}{1 + \frac{r_s}{r}} \left(1 + \frac{r_s}{r}\right) \log\left(1 + \frac{r_s}{r}\right). \quad (15)$$

We now turn to studying the behavior of $f(r)$ and demonstrate its radial dependence in Fig. 1, highlighting how it changes under the DM halo parameters. As can be seen from Fig. 1, the behavior of $f(r)$ reduces to the flat spacetime at larger distances, especially at infinity. Furthermore, the curves are slightly shifted to the right to larger r as the DM halo parameters ρ_s and r_s increase, resulting in the strength of the gravitational potential increasing.

The spacetime Eq. (14) has an event horizon, where a corotating observer's 4-velocity becomes null, resulting from setting $f(r) = 0$. It is then straightforward to obtain the event horizon, r_h , in the form

$$r_h = \frac{r_s}{\frac{4\pi\rho_s r_s^3}{M} W\left(\frac{M \exp\left[\frac{2M+r_s}{8\pi\rho_s r_s^3}\right]}{4\pi\rho_s r_s^3}\right) - 1}, \quad (16)$$

where $W(z)$ is referred to as the Lambert function, defined as the principal solution of $W \exp(W) = z$ for arbitrary z . In Fig. 2, we show the behavior of the event horizon based on the density ρ_s and the characteristic scale r_s of the DM halo. From Fig. 2, one can easily observe that an increase in ρ_s and r_s leads to an increase in the event horizon. It can be seen from Eq. (2) that the DM halo parameters (i.e., ρ_s and r_s) contribute to an increase in mass, enhancing the gravitational potential.

III. THE SPACETIME CURVATURE CHARACTERISTICS AND ENERGY CONDITIONS

Now we analyze the spacetime curvature invariants of a novel Schwarzschild-like BH spacetime metric with a DM halo characterized by a Dehnen-type density profile. To accomplish this, one needs to evaluate the curvature invariants of the spacetime metric, including the Ricci scalar R , Ricci square $R_{\mu\nu}R^{\mu\nu}$, and Kretschmann scalars $R_{\mu\nu\alpha\beta}R^{\mu\nu\alpha\beta}$. To determine whether there is a spacetime singularity or not at $r = 0$, we further examine these fundamental invariants. We begin to analyze the Ricci scalar R , which for this BH-DM spacetime metric reads

as

$$R = \frac{8\pi\rho_s r_s^2 [2\mathcal{N} \log \mathcal{F} - r_s \mathcal{F} \mathcal{M}]}{r^4 \mathcal{F}}. \quad (17)$$

It is obvious that the Ricci-flat for the Schwarzschild case (i.e., $\rho_s = 0$) but it is true in the BH-DM halo system halo. The Kretschmann scalar reads as follows:

$$K = \frac{48M^2}{r^6} + \frac{64\pi M \rho_s r_s^2 \left[\frac{r_s(4r+3r_s)}{(r+r_s)^2} + 2 \log \mathcal{F}\right]}{r^5} + O(\rho_s^2), \quad (18)$$

which reduces to the Schwarzschild case, $K = \frac{48M^2}{r^6}$, when $\rho_s = 0$. Meanwhile, the Ricci square reads as

$$R^2 = \mathcal{A} \left[\mathcal{B} \mathcal{F}^2 + 4r_s^2 r^2 \mathcal{F}^2 \log \mathcal{F} (\mathcal{C} \log \mathcal{F} + \mathcal{D}) - 4r^2 r_s \mathcal{F} \times \mathcal{G} \log \mathcal{F} + \mathcal{H} \log^2 \mathcal{F} \right], \quad (19)$$

Here we note that we use the following notations in Eqs. (17)-(19), which are given by

$$\mathcal{A} = \frac{32\pi^2 \rho_s^2 r_s^4}{r^4 (r + r_s)^6}, \quad (20a)$$

$$\mathcal{F} = 1 + \frac{r_s}{r}, \quad (20b)$$

$$\mathcal{B} = r_s^2 r^2 (4r^2 + 8rr_s + 5r_s^2), \quad (20c)$$

$$\mathcal{C} = (r^2 + 2rr_s + 2r_s^2), \quad (20d)$$

$$\mathcal{D} = 2r^2 + 4rr_s + 3r_s^2, \quad (20e)$$

$$\mathcal{G} = \left[2r^3 + 8r^2 r_s + 2(r^3 + 4r^2 r_s + 5rr_s^2 + 3r_s^3) \right. \quad (20f)$$

$$\left. \times \log \mathcal{F} + 10rr_s^2 + 5r_s^3 \right], \quad (20g)$$

$$\mathcal{H} = 4r^2 (r^4 + 6r^3 r_s + 13r^2 r_s^2 + 12rr_s^3 + 5r_s^4), \quad (20h)$$

$$\mathcal{N} = (r^2 + 3rr_s + 3r_s^2), \quad (20i)$$

$$\mathcal{M} = [2(r + 2r_s) \log \mathcal{F} + 2r + 3r_s]. \quad (20j)$$

From these equations, one can deduce that the spacetime singularity appears at $r = 0$. Furthermore, we show the radial behavior of these curvature invariants in Fig. 3. Also, the behavior of the spacetime singularity is clearly seen in Fig. 3. These curvature invariants, respectively, approach zero and infinity when $r \rightarrow \infty$ and $\rightarrow 0$, i.e.,

$$\lim_{r \rightarrow \infty} R, R_{\mu\nu}R^{\mu\nu}, R_{\mu\nu\alpha\beta}R^{\mu\nu\alpha\beta} \rightarrow 0, \quad (21)$$

and

$$\lim_{r \rightarrow 0} R, R_{\mu\nu}R^{\mu\nu}, R_{\mu\nu\alpha\beta}R^{\mu\nu\alpha\beta} \rightarrow \infty. \quad (22)$$

The energy conditions are also considered to be fundamental characteristics of spacetime, like the curvature invariants. Here, we provide some insight by analyzing the corresponding energy conditions. We then turn to solving Einstein's Eq. (6) together with the energy-momentum tensor $T_\mu^\nu = \text{diag}[-\rho(r), P_r(r), P_\theta(r), P_\phi(r)]$.

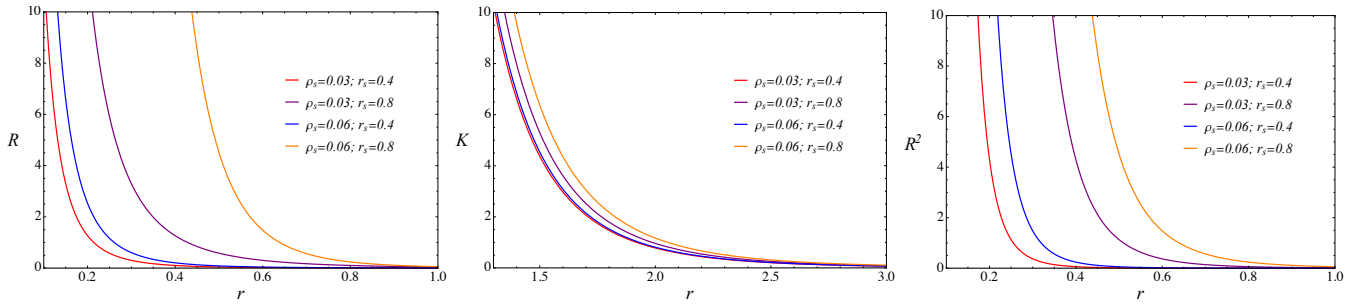


FIG. 3: The Ricci scalar (R) (left panel), the Kretschmann scalar (K) (middle panel), and the square of the Ricci tensor (R^2) (right panel) as a function of r for a Schwarzschild-like BH in a DM halo for varying ρ_s and r_s parameters.

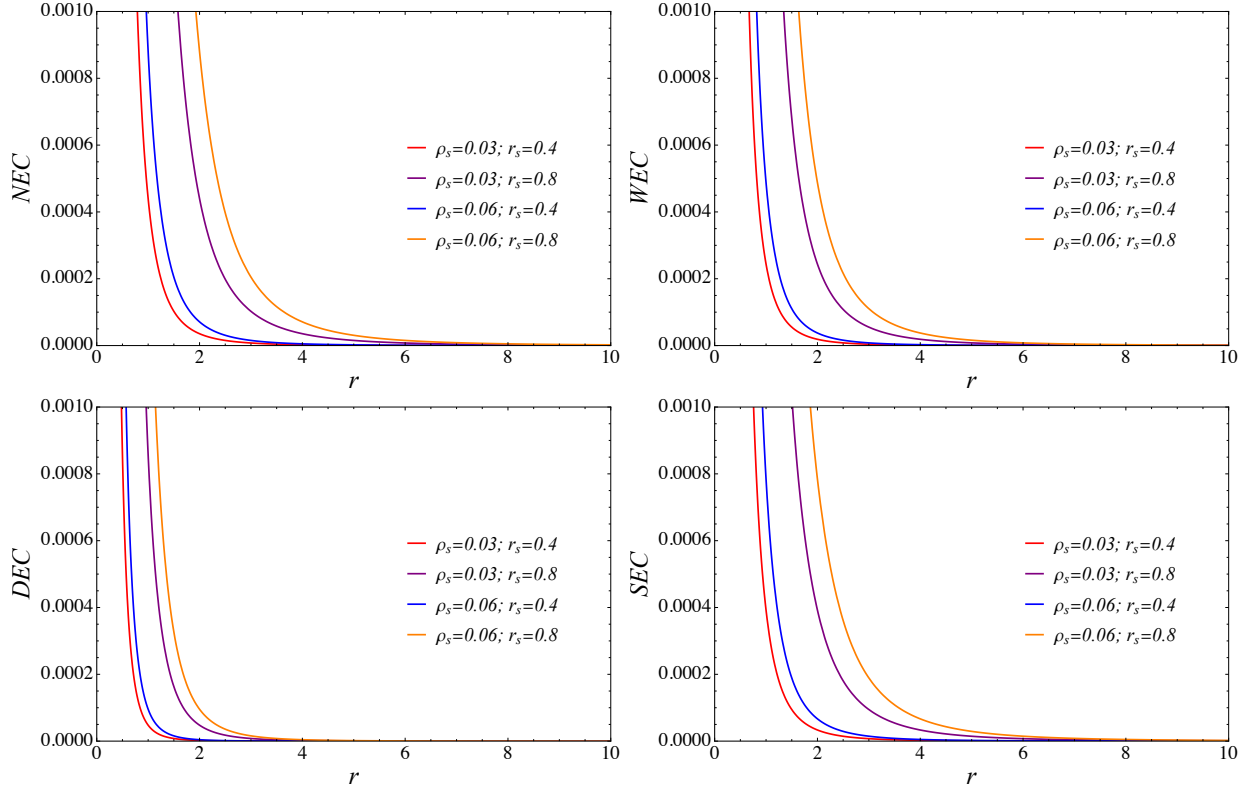


FIG. 4: The radial dependence of the NEC (top left), WEC (top right), DEC (bottom left), SEC (bottom right) for varying ρ_s and r_s parameters.

Consequently, we derive the stress-energy tensor elements as

$$-\rho(r) = P_r(r) = \frac{M_D(r)}{4\pi r^3} \left[1 - \log \left(1 + \frac{r_s}{r} \right)^{\left(1 + \frac{r}{r_s} \right)} \right], \quad (23)$$

$$P_\theta(r) = P_\phi(r) = \frac{M_D(r)r_s}{8\pi r^3(r + r_s)}.$$

Taking the above equations into consideration, we further examine energy conditions for the source fluid. It is worth noting that the stress-energy tensor must satisfy certain inequalities. Therefore, we further consider the null, weak, dominant, and strong energy conditions.

- The null-energy condition (NEC) is a fundamental requirement in GR and plays a crucial role in the study of gravitational physics. It ensures that the energy density associated with matter and fields in spacetime is always positive or zero, preventing the occurrence of exotic phenomena such as negative energy densities or violations of energy conditions. The NEC is a key ingredient in the formulation of the Einstein field equations and is essential for maintaining the consistency and physical viability of the theory. Taken all together, the NEC implies

[34, 49]:

$$T_{\mu\nu}n^\mu n^\nu \geq 0, \quad (24)$$

or

$$\rho(r) + P_i(r) \geq 0, \quad (i = r, \theta, \phi),$$

where n^α is the null vector. One can easily conclude from Eq. (23) that $P_r(r) + \rho(r) = 0$ and:

$$\begin{aligned} \rho(r) + P_\beta(r) &= \frac{\rho_s r_s^3 \left[\log \left(1 + \frac{r_s}{r} \right)^{2r_s \left(1 + \frac{r_s}{r_s} \right)^2} - 2r - r_s \right]}{2r^2 (r + r_s)^2}, \end{aligned} \quad (25)$$

with $\beta = \theta, \phi$. From Eq.(25) it is obvious:

$$\lim_{r \rightarrow 0} [\rho(r) + P_\beta(r)] = \infty, \quad (26)$$

$$\lim_{r \rightarrow \infty} [\rho(r) + P_\beta(r)] = 0.$$

The behavior of the NEC is demonstrated in Fig 4 for various possible cases of the DM halo parameters.

- The weak energy condition (WEC) is also a fundamental requirement in GR and imposes the requirement that the total energy density measured by an observer traversing a timelike curve cannot be negative, which implies [34, 49]:

$$\rho \geq 0, \quad \rho(r) + P_i(r) \geq 0, \quad (i = r, \theta, \phi). \quad (27)$$

We depict the behavior of the WEC in Fig. 4 for various possible cases.

- The dominant energy condition (DEC) states that for any future-directed causal vector field (whether timelike or null), the vector $-T^\mu_\nu \mathbf{Y}^\nu$ must also be a future-directed causal vector. This condition, which is stronger than the WEC, physically implies that the local energy density is non-negative and that energy flux cannot propagate faster than light relative to any local observer. The DEC implies following condition [34]:

$$\rho(r) - |P_{\theta, \phi}| \geq 0, \quad (28)$$

$$\frac{\rho_s r_s^3 \left[2(r + r_s) \log \left[\left(1 + \frac{r_s}{r} \right)^{1 + \frac{r_s}{r_s}} \right] - 2r - 3r_s \right]}{2r^2 (r + r_s)^2} \geq 0.$$

The above equation guarantees the satisfaction of this energy condition. Similar behavior is also shown in Fig. 4 for various possible cases.

- Finally, the strong energy condition (SEC) can be determined by [34]

$$(T_{\mu\nu} - \frac{1}{2} T g_{\mu\nu}) n^\mu n^\nu \geq 0, \quad (29)$$

or

$$\rho + \sum_{i=1}^3 P_i \geq 0,$$

which gives

$$\frac{\rho_s r_s^4}{r^2 (r + r_s)^2} \geq 0. \quad (30)$$

Based on the above analysis of the energy conditions, we obtain compelling results indicating that all energy conditions are well satisfied. This conclusion is further supported by a graphical analysis for the obtained BH spacetime metric within a Dehnen-type DM halo, presented in Eq. 14. Additionally, we present a clear analysis that illustrates the radial behavior of NEC, WEC, DEC, and SEC, as seen in Fig. 4. Both analytical and graphical investigations consistently confirm the validity of all energy conditions.

IV. CONCLUSION

Black holes interact gravitationally with their surrounding environments, making the study of BH-DM systems increasingly important task in astrophysical contexts. It is widely believed that supermassive BHs at the centers of galaxies are embedded in complex, dynamic matter distributions, including DM halos [3, 5–8, 13]. Motivated by this, we derived a novel analytical Schwarzschild-like BH solution, representing a static BH surrounded by a DM halo characterized by a Dehnen-type density profile (1, 4, 2).

We investigated the properties of this BH by analyzing the spacetime curvature properties. Specifically, we computed the curvature invariants of the spacetime metric to determine the presence of singularities. Our results indicated that a spacetime singularity appears at $r = 0$, as illustrated in Fig. 3. We also examined the energy conditions, which are fundamental characteristics of the physical viability of spacetime. Our analysis showed that all energy conditions are well satisfied for the derived BH solution within the Dehnen-type DM halo. This conclusion was further supported by graphical results, as presented in Fig. 4, with analytical and graphical analyzes consistently confirming the validity of all energy conditions.

Our approach offers fundamental astrophysical implications, particularly concerning the significant role of DM halos around supermassive BHs in galactic nuclei. Specifically, the Dehnen-type density distribution used here supports the existence of a BH solution with a DM

halo within the density profile (1, 4, 2). Our finding could offer a novel perspective on the formation of DM halos, providing a potential alternative framework for understanding their fundamental properties.

ACKNOWLEDGEMENTS

S.S. is supported by the National Natural Science Foundation of China under Grant No. W2433018.

-
- [1] B. P. Abbott and et al. (Virgo and LIGO Scientific Collaborations), *Phys. Rev. Lett.* **116**, 061102 (2016), [arXiv:1602.03837 \[gr-qc\]](#).
- [2] B. P. Abbott and et al. (Virgo and LIGO Scientific Collaborations), *Phys. Rev. Lett.* **116**, 241102 (2016), [arXiv:1602.03840 \[gr-qc\]](#).
- [3] K. Akiyama and et al. (Event Horizon Telescope Collaboration), *Astrophys. J.* **875**, L1 (2019), [arXiv:1906.11238 \[astro-ph.GA\]](#).
- [4] K. Akiyama and et al. (Event Horizon Telescope Collaboration), *Astrophys. J. Lett.* **930**, L12 (2022).
- [5] M. J. Rees, *Annu. Rev. Astron. Astrophys.* **22**, 471 (1984).
- [6] J. Kormendy and D. Richstone, *Annu. Rev. Astron. Astrophys.* **33**, 581 (1995).
- [7] F. Iocco, M. Pato, and G. Bertone, *Nature Phys.* **11**, 245 (2015), [arXiv:1502.03821 \[astro-ph.GA\]](#).
- [8] G. Bertone and T. M. P. Tait, *Nature* **562**, 51 (2018), [arXiv:1810.01668 \[astro-ph.CO\]](#).
- [9] V. C. Rubin and J. Ford, W. Kent, *Astrophys. J.* **159**, 379 (1970).
- [10] E. Corbelli and P. Salucci, *Mon. Not. Roy. Astron. Soc.* **311**, 441 (2000), [arXiv:astro-ph/9909252 \[astro-ph\]](#).
- [11] M. Davis, G. Efstathiou, C. S. Frenk, and S. D. M. White, *Astrophys. J.* **292**, 371 (1985).
- [12] M. Persic, P. Salucci, and F. Stel, *Mon. Not. R. Astron. Soc.* **281**, 27 (1996), [arXiv:astro-ph/9506004 \[astro-ph\]](#).
- [13] M. Valluri, D. Merritt, and E. Emsellem, *Astrophys. J.* **602**, 66 (2004), [arXiv:astro-ph/0210379 \[astro-ph\]](#).
- [14] K. Akiyama and et al. (Event Horizon Telescope Collaboration), *Astrophys. J.* **875**, L6 (2019), [arXiv:1906.11243 \[astro-ph.GA\]](#).
- [15] C. Boehm and P. Fayet, *Nucl. Phys. B* **683**, 219 (2004), [arXiv:hep-ph/0305261 \[hep-ph\]](#).
- [16] G. Bertone, D. Hooper, and J. Silk, *Phys. Rep.* **405**, 279 (2005), [arXiv:hep-ph/0404175 \[hep-ph\]](#).
- [17] J. L. Feng, M. Kaplinghat, H. Tu, and H.-B. Yu, *J. Cosmol. Astropart. Phys.* **2009**, 004 (2009), [arXiv:0905.3039 \[hep-ph\]](#).
- [18] M. Schumann, *J. Phys. G Nucl. Part. Phys.* **46**, 103003 (2019), [arXiv:1903.03026 \[astro-ph.CO\]](#).
- [19] S. Babak, J. Gair, A. Sesana, E. Barausse, C. F. Sopuerta, C. P. L. Berry, E. Berti, P. Amaro-Seoane, A. Petiteau, and A. Klein, *Phys. Rev. D* **95**, 103012 (2017), [arXiv:1703.09722 \[gr-qc\]](#).
- [20] D. A. Brown, J. Brink, H. Fang, J. R. Gair, C. Li, G. Lovelace, I. Mandel, and K. S. Thorne, *Phys. Rev. Lett.* **99**, 201102 (2007), [arXiv:gr-qc/0612060 \[gr-qc\]](#).
- [21] P. Amaro-Seoane, *Phys. Rev. D* **98**, 063018 (2018), [arXiv:1807.03824 \[astro-ph.HE\]](#).
- [22] D. Clowe, M. Bradač, A. H. Gonzalez, M. Markevitch, S. W. Randall, C. Jones, and D. Zaritsky, *Astrophys. J. Lett.* **648**, L109 (2006), [arXiv:astro-ph/0608407 \[astro-ph\]](#).
- [23] G. Bertone, D. Hooper, and J. Silk, *Phys. Rep.* **405**, 279 (2005), [arXiv:hep-ph/0404175 \[hep-ph\]](#).
- [24] J. G. de Swart, G. Bertone, and J. van Dongen, *Nature Astron.* **1**, 0059 (2017), [arXiv:1703.00013 \[astro-ph.CO\]](#).
- [25] R. H. Wechsler and J. L. Tinker, *Annu. Rev. Astron. Astrophys.* **56**, 435 (2018), [arXiv:1804.03097 \[astro-ph.GA\]](#).
- [26] D. Merritt, A. W. Graham, B. Moore, J. Diemand, and B. Terzić, *Astron. J.* **132**, 2685 (2006), [arXiv:astro-ph/0509417 \[astro-ph\]](#).
- [27] A. A. Dutton and A. V. Macciò, *Mon. Not. Roy. Astron. Soc.* **441**, 3359–3374 (2014).
- [28] J. F. Navarro, C. S. Frenk, and S. D. M. White, *Astrophys. J.* **462**, 563 (1996).
- [29] A. Burkert, *Astrophys. J.* **447** (1995), 10.1086/309560.
- [30] W. Dehnen, *Mon. Not. R. Astron. Soc.* **265**, 250 (1993).
- [31] Shukirgaliyev, B., Otebay, A., Sobolenko, M., Ishchenko, M., Borodina, O., Panamarev, T., Myrzakul, S., Kalamabay, M., Naurzbayeva, A., Abdikamalov, E., Polyachenko, E., Banerjee, S., Berczik, P., Spurzem, R., and Just, A., *Astron. Astrophys.* **654**, A53 (2021).
- [32] M. M. Gohain, P. Phukon, and K. Bhuyan, *Phys. Dark Univ.* **46**, 101683 (2024), [arXiv:2407.02872 \[gr-qc\]](#).
- [33] R. C. Pantig and A. Övgün, *J. Cosmol. Astropart. Phys.* **2022**, 056 (2022), [arXiv:2202.07404 \[astro-ph.GA\]](#).
- [34] A. Al-Badawi, S. Shaymatov, and Y. Sekhmani, *J. Cosmol. Astropart. Phys.* **2025**, 014 (2025), [arXiv:2411.01145 \[gr-qc\]](#).
- [35] M.-H. Li and K.-C. Yang, *Phys. Rev. D* **86**, 123015 (2012), [arXiv:1204.3178 \[astro-ph.CO\]](#).
- [36] S. Shaymatov, B. Ahmedov, and M. Jamil, *Eur. Phys. J. C* **81**, 588 (2021).
- [37] S. Shaymatov, D. Malafarina, and B. Ahmedov, *Phys. Dark Universe* **34**, 100891 (2021), [arXiv:2004.06811 \[gr-qc\]](#).
- [38] S. Shaymatov, P. Sheoran, and S. Siwach, *Phys. Rev. D* **105**, 104059 (2022), [arXiv:2110.10610 \[gr-qc\]](#).
- [39] V. Cardoso, K. Destounis, F. Duque, R. P. Macedo, and A. Maselli, *Phys. Rev. D* **105**, L061501 (2022), [arXiv:2109.00005 \[gr-qc\]](#).
- [40] X. Hou, Z. Xu, M. Zhou, and J. Wang, *J. Cosmol. Astropart. Phys.* **2018**, 015 (2018), [arXiv:1804.08110 \[gr-qc\]](#).
- [41] Z. Shen, A. Wang, Y. Gong, and S. Yin, *Phys. Lett. B* **855**, 138797 (2024), [arXiv:2311.12259 \[gr-qc\]](#).
- [42] T. Xamidov, U. Uktamov, S. Shaymatov, and B. Ahmedov, *Phys. Dark Universe* **47**, 101805 (2025).
- [43] A. Al-Badawi and S. Shaymatov, *Chin. Phys. C* **49**, 055101 (2025), [arXiv:2501.15397 \[gr-qc\]](#).
- [44] A. Al-Badawi and S. Shaymatov, *Commun. Theor. Phys.* **77**, 035402 (2025).
- [45] M. Alloqulov, T. Xamidov, S. Shaymatov, and B. Ahmedov, *arXiv e-prints*, [arXiv:2504.05236 \(2025\)](#), [arXiv:2504.05236 \[gr-qc\]](#).
- [46] T. Matos and D. Nunez, *Rev. Mex. Fis.* **51**, 71 (2005).

- [47] Z. Xu, X. Hou, X. Gong, and J. Wang, *J. Cosmol. Astropart. Phys.* **2018**, 038 (2018), arXiv:1803.00767 [gr-qc].
- [48] H. Mo, F. C. van den Bosch, and S. White, *Galaxy Formation and Evolution* (Cambridge University Press, Cambridge, 2010).
- [49] B. Toshmatov, C. Bambi, B. Ahmedov, A. Abdujabbarov, and Z. Stuchlík, *European Physical Journal C* **77**, 542 (2017), arXiv:1702.06855 [gr-qc].